THE ASTROPHYSICAL JOURNAL, 197:355–363, 1975 April 15

TEMPERATURE AND EMISSION-LINE STRUCTURE AT THE EDGES OF H II REGIONS

DIPANKAR C. V. MALLIK
Washburn Observatory, University of Wisconsin
Received 1974 June 3; revised 1974 October 14

ABSTRACT

Models of ionization fronts located at the edges of expanding H II regions are presented. These fronts are of the weak D-type and are preceded by shocks in the H I clouds. Since the energy input time is smaller than the cooling time, the gas is found to heat up to a high temperature immediately following ionization. At the trailing edge of the front, the temperature decreases and the ionized gas merges with the main bulk of the nebula where the physical processes are in equilibrium. The emission in [O II] and [N II] lines is greatly enhanced because of the high temperature at the front. The emission in these and other important lines is calculated and compared with Hβ. Effects of different velocities of flow, of different exciting stars, and of different gas densities on the structure of the fronts are also investigated.

Observations of bright rims of H II regions where enhanced emission of [N II] lines has been reported are discussed on the basis of these models.

Subject heading: nebulae

I. INTRODUCTION

H II regions are known to expand into the surrounding H I clouds due to the existence of a pressure gradient across the ionization front (Oort 1954; Kahn 1954; Oort and Spitzer 1955; Savedoff and Greene 1955). The initial expansion produces a shock which propagates into the H I cloud. Behind the shock the density rises as the shock-deposited energy is dissipated in the form of radiation. Inside the ionized volume the decrease in density due to the expansion makes more ionizing photons available, and the ionization front moves outward following the shock. After a time short compared with the lifetime of the H II region the cloud settles down to the following configuration: (i) an ionized volume of gas where equilibrium conditions prevail: (ii) a transition region, the ionization front, where dynamical effects are important; (iii) a shocked shell of neutral matter cooled to its preshock temperature into which the ionization front is moving; (iv) a shock front ahead of this neutral shell; and (v) an undisturbed H I region outside the shock front. The entire configuration grows in size until the exciting star evolves off the main sequence. This picture assumes an infinite extent for the cloud.

Since the expansion of an H II region lasts for a longer time than the typical time scales of recombination and cooling in a dilute gas, at the trailing edge of the ionization front (adjacent to the equilibrium H II region) the gas is nearly in a state of equilibrium while in the ionization front and at the leading edge (close to the dense neutral matter) large deviations from equilibrium conditions may occur. For a mature H II region, i.e., one with its age large compared with the formation time (Mathews and O'Dell 1969), the acceleration of the ionization front itself is negligible, and in a frame of reference moving with the ionization front the structure of the front can be assumed to be stationary.

Observations of the emission lines in H II regions have provided valuable information on the physical nature of the ionized gas, its distribution and kinematical properties within the nebula. Depending on the physical conditions and the distribution, certain lines are enhanced in certain parts of the nebula. In particular, the [N II] lines $\lambda\lambda$6548, 6583 have been found enhanced near the bright rim structures observed in many of these nebulae (Courtès, Louise, and Monnet 1968, 1969; Foukal 1969; Louise and Sapin 1973; Bohuski 1973). These lines have been extensively used along with Hα to investigate the thermal condition, the turbulence, and the abundance of nitrogen in diffuse nebulae. The ratio $I(\lambda6583)/I(\mathrm{H}\alpha)$ has been found to increase toward the edges of these nebulae. Since Hα is a recombination line and depends weakly on temperature whereas the [N II] λ6583 is collisionally excited and involves a Boltzmann factor, the high value of $I(\lambda6583)/I(\mathrm{H}\alpha)$ has often been interpreted as the evidence of high temperature at the rims.

Equilibrium models of H II regions (Hjellming 1966; Rubin 1968) do show a rise in temperature in the outer parts. However, because of the expansion the outer parts deviate significantly from equilibrium conditions (Mathews 1965), and a proper understanding of the physical conditions near the edge of an H II region requires the application of a dynamical theory to ionization fronts. The peculiar behavior of the [N II] lines near the bright rims is to be understood in the light of such a theory.

We present models describing the ionization, the thermal and the emission-line structure of ionization fronts surrounding H II regions which are beyond their initial phase of expansion. We have assumed a steady

flow in the comoving frame of the ionization front. Similar models were computed by Hjellming (1966). These were limited by the then existing knowledge of the physical processes in gaseous nebulae. No attempt was made in this earlier work to obtain the emission-line structure near the edge. We shall find that the results of the present models are notably different from these earlier models.

We have included hydrogen, helium, oxygen, and nitrogen as the basic constituents of the H II region. Of the other light elements, doubly ionized neon is an important source of cooling in an H II region but theoretically very little of it is expected in the vicinity of an ionization front. Carbon has also been left out because both the singly and the doubly ionized species of carbon are unimportant in cooling processes. The heavy elements do not contribute to the opacity either, owing to their relatively low abundances. For simplicity dust and magnetic forces are also left out of the present models.

II. THEORY

We consider a frame of reference moving with the ionization front. In this frame neutral gas is flowing in at the leading edge of the front, is getting ionized, and is merging into the equilibrium region at the trailing edge. The structure of the front is assumed to be stationary in this comoving frame. Since the spatial extent of the ionization front is small compared with the size of the H II region itself, its curvature is neglected and the front is assumed to have plane-parallel symmetry.

The flow of the gas through the ionization front is described by

$$\frac{d}{dz}(\rho u) = 0\,, \tag{1}$$

$$u\frac{du}{dz} + \frac{1}{\rho}\frac{dp}{dz} = 0\,. \tag{2}$$

Here u denotes the velocity of an element of gas in the moving frame of the front, ρ the density of the gas, and p its pressure. The quantities ρ and p can be expressed in terms of the number densities of hydrogen and helium $N_{\rm H}$, $N_{\rm He}$, their fractional ionization x and y, and the temperature T of the gas (Hjellming 1966):

$$\rho = m_{\rm H}N_{\rm H} + m_{\rm He}N_{\rm He}\,, \tag{3}$$

$$p = (1 + x)N_{\rm H}kT + (1 + y)N_{\rm He}kT\,. \tag{4}$$

The physical processes in the front are dominated by the absorption by the gas of the stellar photons of energy larger than or equal to the Lyman threshold energy. For a plane-parallel ionization front, the mean intensity of stellar radiation at any point in the front is given by

$$4\pi J_\nu^s(z) = 4\pi J_\nu^s(z = 0)\exp\left(-\int_0^z k_\nu dz'\right), \tag{5}$$

where k_ν is the absorption per unit length. The point $z = 0$ corresponds to a distance r from the star, close to the Strömgren radius for the static H II region with the given star and density.

Because of their high abundances, hydrogen and helium are the main sources of opacity in a nebula. The differential monochromatic optical depth is given by

$$d\tau_\nu = [N_{\rm H^0}a_\nu({\rm H}) + N_{\rm He^0}a_\nu({\rm He})]dz\,, \tag{6}$$

where a_ν(H) and a_ν(He) are the ground-state photoionization cross sections of hydrogen and helium, respectively, and $N_{\rm H^0}$, $N_{\rm He^0}$ are the number densities of hydrogen and helium atoms. If the optical depths at the Lyman and He I thresholds be denoted by $\tau_{\rm H}$ and $\tau_{\rm He}$ and the corresponding frequencies by ν_0 and ν_2, respectively, τ_ν can also be written as

$$\tau_\nu(z) = \frac{a_\nu({\rm H})}{a_{\nu_0}({\rm H})}\tau_{\rm H}(z) + \frac{a_\nu({\rm He})}{a_{\nu_2}({\rm He})}\tau_{\rm He}(z)\,. \tag{7}$$

The ionizations of hydrogen and helium are determined from

$$\frac{d}{dz}(uN_{\rm H^+}) = -N_{\rm H^0}\int_{\nu_0}^{\infty}\frac{4\pi J_\nu}{h\nu}a_\nu({\rm H})d\nu - 0.964N_{\rm He^+}N_e\alpha_B({\rm He}) + N_{\rm H^+}N_e\alpha_B({\rm H})\,, \tag{8}$$

$$\frac{d}{dz}(uN_{\rm He^+}) = -N_{\rm He^0}\int_{\nu_0}^{\infty}\frac{4\pi J_\nu}{h\nu}a_\nu({\rm He})d\nu + N_{\rm He^+}N_e\alpha_A({\rm He})\,, \tag{9}$$

where J_ν denotes the mean intensity of radiation including a diffuse component due to recombinations to the ground state of helium, N_e is the electron density, and α_B(H), α_A(He), α_B(He) are the recombination coefficients with the subscripts A and B respectively denoting whether recombinations to the ground level of the atoms are included or not. In equation (8) we have taken into account the ionization of hydrogen by the recombination line radiation of helium and have used the "on the spot" approximation for the absorption of diffuse radiation from ground-state recombinations of hydrogen and helium (Hummer and Seaton 1964; Osterbrock 1971).

It is important to know the ionization structure of oxygen and nitrogen because of the different cooling efficiencies of their various ions. Oxygen can be doubly ionized in an H II region while nitrogen can be triply ionized. There is a negligible amount of N^{+3} in an ionization front; hence only two stages of ionization of each of these elements are considered.

The process $O^0 + H^+ \rightleftharpoons O^+ + H^0$ is resonant, and the charge-exchange cross sections is very large. It has been found that even in an H II region charge exchange with protons dominates over the photoionization of O^0. Moreover, since the charge-exchange relaxation length is very small, the ionization of O^0 at any point in the front is determined by the

local ionization of hydrogen. Following Field and Steigman (1971) and also Brown (1972), we write

$$\frac{N(O^+)}{N(O^0)} = \frac{8}{9}\frac{N_{H^+}}{N_{H^0}} . \quad (10)$$

The relative concentration of O^{++} at any point in the front is determined from

$$\frac{d}{dz}[uN(O^{++})] = -N(O^+)\int_{2.59\nu_0}^{\infty}\frac{4\pi J_\nu^s}{h\nu}a_\nu(O^+)d\nu + N(O^{++})N_e\alpha(O^+) . \quad (11)$$

Steigman, Werner, and Geldon (1971) have calculated the charge-exchange cross sections and rate coefficients for charge exchange between protons and N^0 atoms. For temperatures and densities of interest in nebular work, the rate coefficients are found to be larger than the radiative recombination rates. The fractional ionization of N^0 is then given by

$$\frac{N(N^+)}{N(N^0)} = \frac{R(NH^+)}{R(N^+H)}\frac{N_{H^+}}{N_{H^0}} , \quad (12)$$

where $R(NH^+)$ and $R(N^+H)$ are the rate coefficients for charge exchange between N^0 atoms and protons and between N^+ ions and hydrogen atoms, respectively. The concentration of N^{++} is determined from an equation similar to (11). The thermal structure of the ionization front is calculated from

$$\rho\frac{dQ}{dt} = \rho\frac{dU}{dt} + \rho p\frac{dV}{dt} , \quad (13)$$

where U denotes the internal energy per gram, V the specific volume, and Q the total energy per gram of material. The ionization energy is subtracted out of Q and hence is not included in U. The left-hand side of equation (13) equals $\Gamma - \Lambda$ where Γ is the energy gain in ergs cm^{-3} s^{-1} and Λ the energy loss in the same units. Equation (13) can be simplified with the help of (2) to

$$pu\frac{d}{dz}\left(U + \frac{p}{\rho} + \frac{1}{2}u^2\right) = \Lambda - \Gamma , \quad (14)$$

where we have replaced d/dt by $-ud/dz$. The internal energy U is given by

$$U = \frac{3}{2}\frac{(1 + x) + (1 + y)A}{m_H + m_{He}A}kT ,$$

where A is the abundance of helium by number with respect to hydrogen.

Evaluation of Γ and Λ has been discussed extensively in literature (Spitzer 1948, 1949; Spitzer and Savedoff 1950; Burbidge, Gould, and Pottasch 1963). In the present work the heating through the ionization by diffuse radiation of helium has also been included in Γ.

The surface fluxes of the ionizing stars are taken from the model atmospheres of Hummer and Mihalas (1970). The radii are obtained from Morton's (1969) data on O stars in conjunction with Morgan's (1972) calibration of the spectral type and M_v for these stars. The photoionization cross sections have been obtained from Bethe and Salpeter (1957), Bell and Kingston (1967), and Henry (1970). Many of the collision strengths used for the computation of collisional excitation have come from the work of Saraph, Seaton, and Shemming (1969). Radiative recombination coefficients are determined by using the expressions of Seaton (1959) for all except helium for which the data of Brown and Mathews (1971) have been fitted to suitable formulae. For computation of the line strengths we have used the atomic data of Pengelly (1964) and Brocklehurst (1971, 1972).

The structure of the ionization front is determined by the stellar flux incident at the trailing edge and by physical conditions in the neutral gas ahead which have been modified by the shock progressing into the undisturbed material. Unfortunately there is no simple way of relating the strength of the shock to the type of the star and the initial density. The upstream conditions are determined by the previous dynamical history of the nebula. The velocity of the gas as it emerges from the trailing edge of the front is related to the upstream conditions through the equation of continuity and cannot be known *a priori*. This velocity, denoted by u_{i2}, is taken as an input parameter in the present problem.

Beyond the initial phase of expansion when the shock has separated appreciably from the ionization front, the ionization front is of the weak D-type in which the flow is subsonic both ahead of and behind the front (Mathews and O'Dell 1969). From a consideration of time scales, an H II region is supposed to have a weak D-type ionization front for the major part of its life. Hence the models described in the present work all refer to weak D-type ionization fronts.

Given a star and a gas density, it is possible to compute the model of an equilibrium H II region. Since the dynamical effects are important in the outer parts of a nebula, the equilibrium parameters at the very edge would in general be different from the values obtained from a dynamical model. However, at the trailing edge this difference is not very large and cannot propagate very far into the H II region, since the dynamical calculations (Mathews 1965) indicate that the bulk of an H II region can be described rather well by equilibrium models. We start the calculation by considering a point in the H II region, not far from the edge. We then assume reasonable values for the optical depths at the Lyman threshold and at the He I threshold at this point. It is then possible to calculate the temperature and ionization by solving the equations of ionization and thermal equilibria. A guess at the velocity u_{i2} then gives a sufficient number of initial conditions to numerically integrate the equations of the front. Depending on the choice of u_{i2}, the integration across the front yields different values of temperatures and densities for the neutral gas where the ionization goes to zero. Since the upstream density

and temperature are not specified, there is a range of values of u_{i2} that gives acceptable solutions for a weak D-type ionization front.

We integrate the dynamical equations "backwards" (i.e., toward the star) and obtain values of the physical variable at an inner point. These values are better than the original, rather arbitrary, guesses because the solutions relax towards the equilibrium solution in the backward integration. We then start from this inner point ($z = 0$) and integrate forward to obtain the structure of the ionization front. The boundary conditions at the leading edge are not specified by any fixed value of temperature or of the velocity u_{i2} but we do require $x \to 0$, $y \to 0$, and $T \to 0$ at the leading edge. It is also required that the velocity at the leading edge be less than the local sonic velocity. For an integration that does not satisfy these conditions the whole procedure is repeated with a different choice of the optical depths and u_{i2}. A second-order predictor-corrector scheme is used for the integration of the differential equations.

The origin of the spatial coordinate z corresponds to the starting point of the final integration for any model. In reality it corresponds to a position r_0 close to the outer edge of an H II region. The flux at this point can only be computed when r_0 and hence the spatial dilution of the radiation is specified. The optical depths τ_H and τ_{He} are also functions of this distance but their dependence on r_0 is weak since the gas in the H II region is almost completely ionized, and it is only at the edge that the optical depths start increasing very rapidly. For all the models to be discussed r_0 has been chosen to correspond to $0.9R_s$, where R_s is the Strömgren radius of the H II region.

III. RESULTS

Table 1 summarizes the models computed in the present program. The abundances chosen for all the models except model 7 are $N(\mathrm{He})/N(\mathrm{H}) = 10^{-1}$, $N(\mathrm{O})/N(\mathrm{H}) = 10^{-3}$, and $N(\mathrm{N})/N(\mathrm{H}) = 10^{-4}$. In model 7, the helium and oxygen abundances are kept the same but the nitrogen abundance is increased to 6×10^{-4}.

We now discuss the main features of a typical model. Figure 1 shows a plot of the hydrogen and helium ionization for model 2. The exciting star would be far to the left in the diagram, and the shock is to the right. The decrease in the ionization is smooth, the changes being rather sharp near the leading edge. The thickness of the ionization front is approximately equal to the mean free path of an ionizing photon. In the frame of reference of the ionization front the gas is flowing in toward the star while the distance is taken to be increasing away from the star. Since the ionization front is moving into the neutral material ahead of it, ionizations dominate over recombinations at all points in the front. It is seen that helium is less ionized than hydrogen in the front regions. This is true for all the models. In figures 2 and 3 the ionization structures of oxygen and nitrogen are shown. O^{++} and N^{++} are present in the front regions in almost equal amounts. These species recombine to O^+ and N^+, respectively, going upstream from the trailing edge of the front. As a result initially fractions of both O^+ and N^+ increase reaching maximum values where O^{++} and N^{++} disappear. Since O^+ and N^+ are tied to the local ionization of hydrogen through charge exchange, their ionization structure follows closely that of hydrogen.

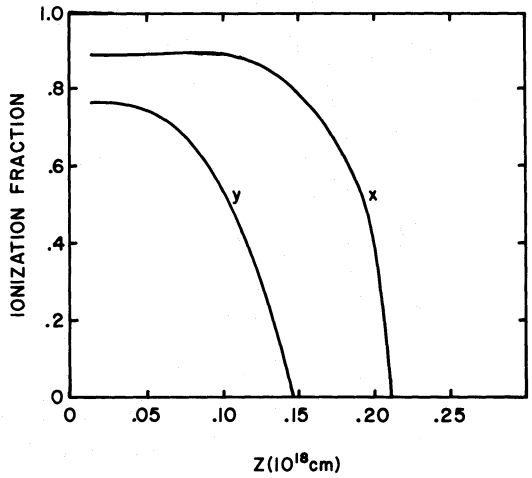

FIG. 1.—The ionization structure of H and He for model 2 ($T_{\mathrm{eff}} = 50{,}000$ K, $N_H = 10\ \mathrm{cm}^{-3}$, $u_{i2} = 2.5\ \mathrm{km\ s}^{-1}$).

Figure 4 shows that the temperature in the front shows a great deal of variation, reaching values of

TABLE 1

MODEL PROPERTIES

MODEL NO.	EFFECTIVE TEMPERATURE OF THE IONIZING STAR (K)	GAS DENSITY IN THE NEBULA (cm^{-3})	u_{i2} ($\mathrm{km\ s}^{-1}$)	THRESHOLD OPTICAL DEPTHS	
				τ_H^i	τ_{He}^i
1.....	40,000	10	2.0	7.6	2.0
2.....	50,000	10	2.5	8.6	5.5
3.....	40,000	10	3.0	7.6	2.0
4.....	40,000	10	4.0	7.7	2.1
5.....	40,000	100	2.5	8.7	3.8
6.....	50,000	100	2.5	10.9	6.6
7.....	40,000	100	3.0	8.3	3.7

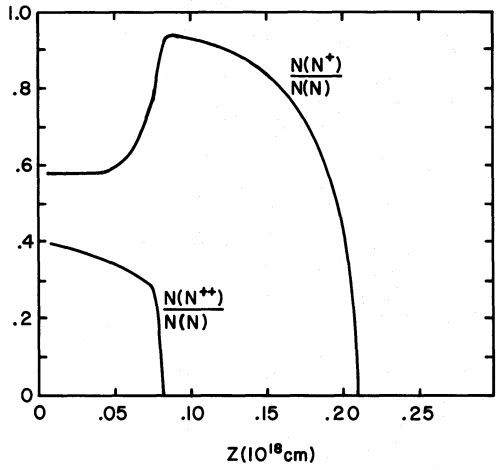

FIG. 2.—Nitrogen ionization structure for model 2

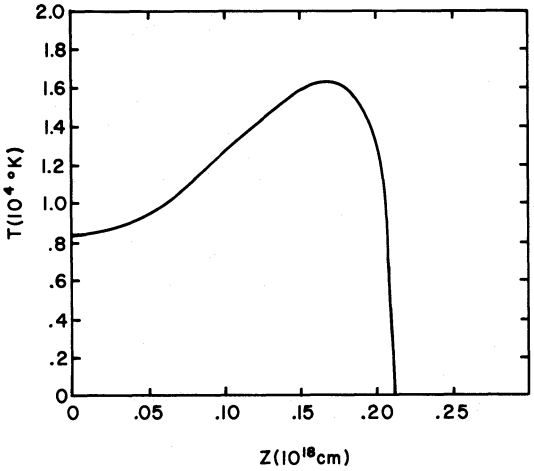

FIG. 4.—Temperature structure for model 2

14,000–16,000 K slightly behind the leading edge and decreasing slowly to near equilibrium values at the trailing edge. It might be suspected that the very high maximum temperature is caused by the hardening of the stellar radiation by preferential nebular absorption of the softer photons. However, this effect is not important: a model was calculated with only one frequency group at $1.80\,\nu_0$. Its thermal structure was about the same as the corresponding multifrequency model.

Instead, the high-temperature peak occurs because the heating by photoionization takes place simultaneously with the ionization, while the cooling must wait for the cooling ions (primarily O^+) to be excited to the upper level of the transition before the emission of the cooling [N II] and [O II] radiation can take place. The distance over which the temperature is high is approximately equal to the cooling length, or the distance which a parcel of gas moves in the average time required for an O^+ ion to be excited from ^4S to the ^2D levels. The temperature peak is made very pronounced by the fact that oxygen is only ionized to O^+ rather than O^{++}, and O^+ has no fine-structure levels which can cool even at low temperature.

The temperature structure in the front is dependent on the velocity u_{i2} and hence on the velocity of the gas. This is shown in figure 5, where the thermal structures for models 1, 3, and 4 have been shown. Each curve is labeled by the value of u_{i2} in km s^{-1}. A larger velocity decreases the temperature gradient and stretches the front but does not change the maximum temperature or the sharpness of the drop at the leading edge. This dependence of the temperature structure on the flow velocity can be explained again in terms of the cooling length defined before. The maximum temperature reached near the leading edge is determined only by the radiation field in that region. Since the field is independent of the velocity u_{i2}, the gas is initially heated to the same temperature.

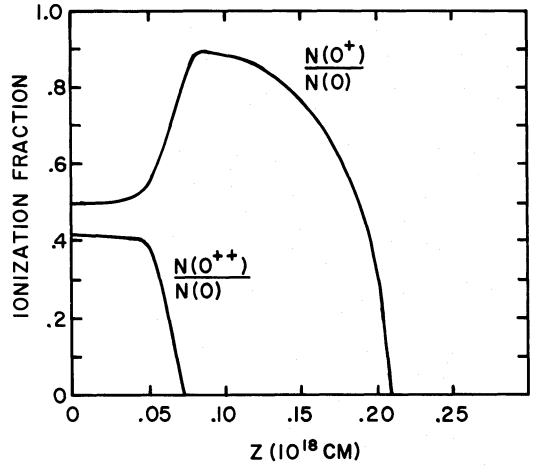

FIG. 3.—Oxygen ionization structure for model 2

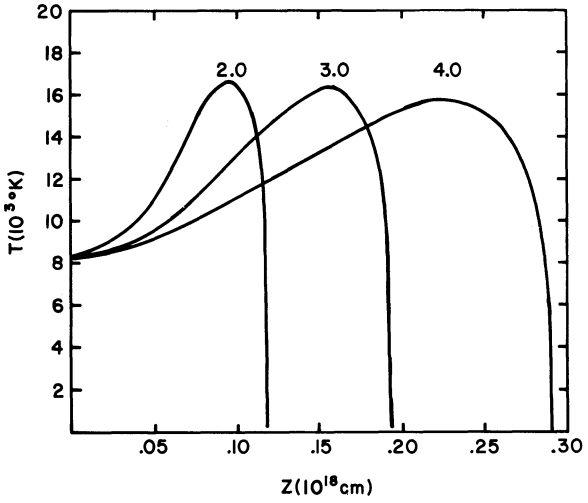

FIG. 5.—Dependence of the temperature on the velocity of flow. Temperature structure for models 1, 3, and 4. Each curve is labeled by u_{i2} in km s^{-1}.

The cooling length is increased because the gas is flowing with a higher velocity in the moving frame.

Figure 6 shows a plot of the pressure, the total density, and the velocity u. For a weak D-type front u is restricted to less than the sonic velocity at all points in the front. If a high u_{i2} were used as an input, the increase in u in the front would make it larger than the sonic velocity at some point in the integration. This would invalidate a weak D front. When the velocity approaches $(5p/3\rho)^{1/2}$ the adiabatic sound velocity, the steady flow approximation scheme used in this paper breaks down because shocks within the ionization front have not been allowed. We restricted the choice of u_{i2} such that this limit was never approached. As the gas enters the leading edge of the front there is a steep fall in the density as the temperature increases. The density of the neutral gas adjacent to the leading edge of the front is orders of magnitude higher than in the H II region. Since most of the change in the density takes place where the ionization is low, the electron density in a parcel of gas shows a smooth increase as it flows through the front into the H II region.

The total pressure p shows very little variation in the front. The freshly ionized gas cools off approximately isobarically. Similar results were obtained by Field *et al.* (1968) for shock fronts in the interstellar medium.

The stellar flux undergoes a redistribution in frequencies as it penetrates further and further into the H II region. The flux reaching the front is peaked at very high frequencies. A comparison of the models 1 and 2 shows that the peculiarities of the stellar flux distribution are washed out by the time the radiation reaches the front regions. The structure of the fronts for the two different exciting stars is very similar. The properties of H II regions generally change with the exciting star. This change is seen in the bulk of the nebula. Even though the ionization front structure is not sensitive to the change in the input radiation field, the H II regions surrounding stars with different effective temperatures are different from one another.

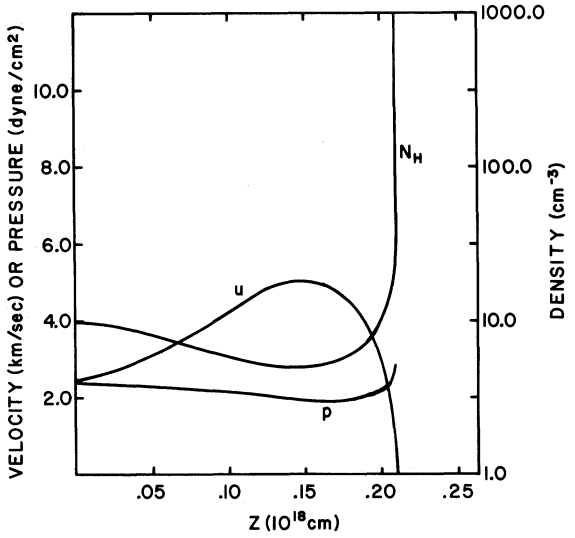

FIG. 6.—Pressure, density, and velocity for model 2. The left ordinate gives u in km s^{-1} and p in 10^{-11} dynes cm^{-2}. The right ordinate gives N_H in cm^{-3}.

The abundance of the important cooling sources affects the thermal structure of the front significantly. In model 7 with a higher nitrogen abundance the cooling is increased and the temperature at the trailing edge is much lower. The average temperature in the front is decreased by about 4000 K. Trial integrations with reduced oxygen and nitrogen abundances produced very high temperatures.

An H II region with a higher density has a thinner ionization front. The models with $N_H = 100$ cm^{-3} are similar to the low-density models in all respects. The collisional de-excitation of the metastable levels of O^+ and N^+ is marginal at this density, and the temperature structure is hardly affected.

The emission-line structure of the ionization fronts is notably different from the equilibrium case. Because of the high temperature attained in the fronts the collisionally excited lines are enhanced with respect to the recombination lines of hydrogen. For exciting stars with high effective temperatures ($T_* \geq$ 40,000 K) both O^+ and N^+ are concentrated in the outer parts of the nebula. The [O II] and [N II] lines have their peak emissions in the ionization front region. Lines of the neutral species O^0 and N^0 can only be emitted in the transition region since they require the presence of both neutrals and electrons for their formation. In models of equilibrium H II regions (Rubin 1968) the [O I] and [N I] lines are extremely weak. The entire emission in these lines is confined to the front regions. Both the [O I] λ6300 and the [N I] λ5202 have emission peaks close to the leading edge of the ionization front (fig. 7).

The column emissivities (tables 2 and 3) are obtained by integrating the computed volume emissivities over the thickness of the ionization front for any model. The line strengths do not include any significant portion of the equilibrium H II region adjacent to the front itself. The first four columns of table 2 may be compared to see the effects of a change of the velocity u_{i2} on the emissivities. In model 4 the emissions in absolute units are increased compared with model 1 because of the larger spatial extent of the ionization front. Since this is a scaling effect, the strengths of the lines with respect to Hβ are hardly changed. The last two columns show the results for the hotter star. In general the strengths of the lines are not changed significantly with a change in the input radiation field except for the ratio [O III] λ5007/[O II] λ3729. For the hotter star the ratio is understandably larger. In all the models the [O II] lines $\lambda\lambda$3726, 3729 are the very strongest. The [O III] and [N II] lines are also quite strong.

The unusual strength of the [O II] lines is not surprising at all since these lines are generally stronger than Hα in the observations of H II regions. Since O^+ is theoretically expected to be concentrated in the outer parts of an H II region, while the hydrogen recombination lines are emitted by the entire nebula,

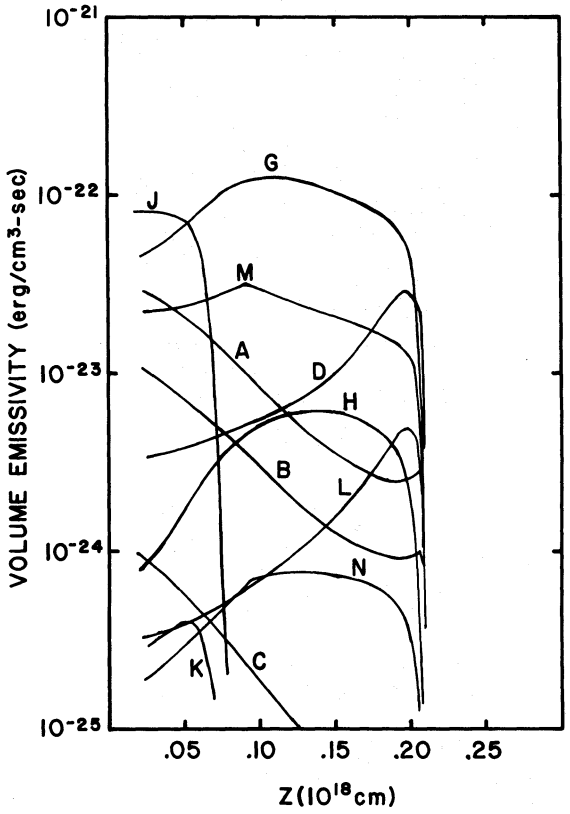

FIG. 7.—Volume emissivities in the important optical lines for model 2. The curves are lettered as follows: A, H I λ6563; B, H I λ4861; C, He I λ5876; D, [O I] λ6300; G, [O II] λ3729; H, [O II] λ7325; J, [O III] λ5007; K, [O III] λ4363; L, [N I] λ5202; M, [N II] λ6584; N, [N II] λ5755.

in reality the [O II] lines will not appear as strong when integration over a significant volume of the nebula is considered. The same argument applies to the [N II] lines which are, in general, a fraction of the strength of Hα in most nebular observations.

The calculated line strengths all refer to the narrow region immediately behind the ionization front. In an observational program it is very difficult to concentrate only on this region, and all observations include some cooler inner parts of the H II region where the physical processes are in equilibrium. Various lines of sight of observations include varying proportions of the inner bulk of the nebula; hence the strength of the [O II] and [N II] lines would vary greatly in scans across an H II region. Published observations by Peimbert and Costero (1969) where line intensities were measured in the different parts of several H II regions show the enhancement of the [O II] and [N II] lines in the outer regions quite clearly. The observations of the ratio [N II]/Hα also bears this out.

The [N II] λ5755 is weak even at the high temperatures of the front regions, although for the brightest H II regions this line should have measurable counts. If this line could be measured, it would provide an excellent test of the temperature increase at the fronts. It is to be noted that in the ionization front the temperature derived from $I(\lambda5007 + \lambda4959)/I(\lambda4363)$ will always be lower than the value derived from $I(\lambda6548 + \lambda6584)/I(\lambda5755)$. The [N II] λ5755 is generally stronger than the [O III] λ4363 in these models.

The hypothesis of a high nitrogen abundance causing an enhancement of the [N II] lines has been put to test in model 7. It has been shown that most of the nitrogen in an ionization front is in N^+. The value of 6×10^{-4} for the nitrogen abundance was derived by Courtès *et al.* (1969) from the [N II]/Hα ratio in IC 434. Interference filter photographs show that the distributions of hydrogen and N^+ in this nebula are very similar. In model 7 the increased cooling due to an increased nitrogen abundance makes the average temperature of the front lower than in the other cases. But the [N II] lines are much stronger than Hα, the integrated ratio λ6583/Hα being

TABLE 2

EMISSIVITIES IN THE LINES FOR THE MODELS WITH $N_H = 10\ cm^{-3}$

		Model 1 (T_{eff} = 40,000 K, u_{i2} = 2 km s^{-1})		Model 4 (T_{eff} = 40,000 K, u_{i2} = 4 km s^{-1})		Model 2 (T_{eff} = 50,000 K, u_{i2} = 2.5 km s^{-1})	
Line	λ(Å)	Emission (10^{-7} ergs cm^{-2} s^{-1} sr^{-1})	Emission Normalized to Hβ	Emission (10^{-7} ergs cm^{-2} s^{-1} sr^{-1})	Emission Normalized to Hβ	Emission (10^{-7} ergs cm^{-2} s^{-1} sr^{-1})	Emission Normalized to Hβ
H I.....	6563	1.383	2.76	2.540	2.76	1.817	2.76
H I.....	4861	0.501	1.00	0.920	1.00	0.658	1.00
He I.....	5876	0.045	0.09	0.074	0.08	0.046	0.07
He I.....	4471	0.020	0.04	0.037	0.04	0.020	0.03
[O III].....	5007	2.009	4.01	3.478	3.78	3.706	5.63
	4363	0.010	0.02	0.018	0.02	0.019	0.03
[O II].....	3729	9.721	19.40	19.450	21.14	12.940	19.65
	7325	0.396	0.79	0.764	0.83	0.546	0.83
[O I].....	6300	0.832	1.66	1.960	2.13	0.994	1.57
	5577	0.040	0.08	0.092	0.10	0.046	0.07
[N II].....	6583	2.370	4.72	5.144	5.59	3.514	5.34
	5755	0.050	0.10	0.110	0.12	0.079	0.12
[N I].....	5202	0.167	0.33	0.405	0.44	0.204	0.31

TABLE 3

EMISSIVITIES FOR THE MODELS WITH $N_H = 100\ cm^{-3}$

LINE	λ*	MODEL 5 (T_{eff} = 40,000 K, u_{i2} = 2.5 km s^{-1}) Emission (10^{-6} ergs cm^{-2} s^{-1} sr^{-1})	MODEL 5 Emission Normalized to Hβ	MODEL 6 (T_{eff} = 50,000 K, u_{i2} = 2.5 km s^{-1}) Emission (10^{-6} ergs cm^{-2} s^{-1} sr^{-1})	MODEL 6 Emission Normalized to Hβ	MODEL 7 (T_{eff} = 40,000 K, u_{i2} = 3.0 km s^{-1}) Emission (10^{-6} ergs cm^{-2} s^{-1} sr^{-1})	MODEL 7 Emission Normalized to Hβ
H I.....	6563	1.715	2.76	1.780	2.76	1.829	2.76
H I.....	4861	0.622	1.00	0.645	1.00	0.663	1.00
He I.....	5876	0.048	0.08	0.046	0.07	0.049	0.07
He I.....	4471	0.022	0.04	0.021	0.03	0.022	0.03
[O III].....	5007	2.752	4.42	7.660	11.88	1.230	1.86
	4363	0.014	0.02	0.054	0.08	0.003	0.01
[O II].....	3729	10.270	16.50	12.880	19.97	4.361	4.52
	7325	0.386	0.62	0.627	0.97	0.106	0.16
[O I].....	6300	0.610	0.98	0.897	1.39	0.497	0.75
	5577	0.026	0.04	0.049	0.08	0.0126	0.02
[N III].....	57 μ	0.228	0.37	0.290	0.45	1.281	1.93
[N II].....	6583	2.892	4.65	2.141	3.32	10.70	16.14
	5755	0.055	0.09	0.057	0.09	0.118	0.18
	204 μ	0.031	0.05	0.035	0.05	0.203	0.31
	122 μ	0.105	0.17	0.111	0.17	0.664	1.00
[N I].....	5202	0.117	0.19	0.193	0.30	0.522	0.78

* In angstroms unless otherwise noted.

as large as 6.0. Figure 8 shows that for our model 2 with normal abundance of nitrogen the ratio of the volume emissivities j_{6583}/j_{6563} varies between 1.0 and 6.0 in the ionization front. The integrated ratio is 1.9. Recently Louise and Sapin (1973) have measured the variation of [N II]/Hα at different points of IC 434 and found an increase of the ratio near the bright rim of this nebula. While their observation may not have isolated the ionization front completely, the maximum values obtained by them lie close to 1.5. It seems likely, therefore, that the enhancement of the [N II] line in this case is due to the temperature increase rather than to an overabundance of nitrogen.

The He I lines at λλ5876, 4471 are very weak in the front regions owing to the low ionization of helium. The [O I] and [N I] lines are quite strong. These lines are emitted in the transition region where O^+ and N^+ are recombining and the temperature is still quite high. The [O I] λ6300 is stronger than Hβ though not as strong as Hα in these models. For the assumed normal abundances the [N I] λ5202 (stronger of the doublet) is one-fifth the strength of the [O I] line. In model 7, the effect of an overabundance of nitrogen is to make λ5202 as strong as λ6300.

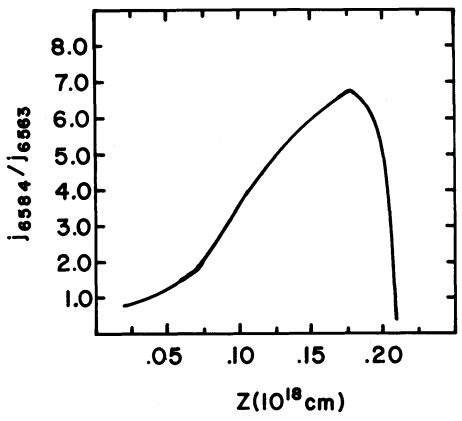

FIG. 8.—Ratio of volume emissivities j_{6583}/j_{6563} in the ionization front for model 2.

The present models show that in the ionization front the [O II] and [N II] emissions are very intense. They provide the major energy sink near the edges of H II regions. Naturally, the ratio [O II] λ3729/[N II] λ6583 appears as an indicator of the oxygen to nitrogen ratio. For the normal abundances this ratio lies between 3.0 and 4.0 while for model 7 it is less than 1.0.

IV. CONCLUSION

A consideration of the dynamics in the vicinity of an ionization front shows that the temperature can reach high values, causing an enhancement of the collisionally excited lines with respect to the less temperature-sensitive hydrogen recombination lines. The observed enhancement of the [N II] lines at the bright rims of H II regions can thus be explained on the basis of dynamical effects. A reduction of the abundances of the cooling ions or an increase of the density may increase the temperature such that collisional ionization of the gas becomes a possibility. This aspect needs further investigation. For fruitful comparison with observations, it is necessary to calculate the expected integrated spectrum of an H II region. A combination of a dynamical model of the edge and an equilibrium model of the inner portion of an H II region is deemed essential for such an evaluation of the spectrum. Equilibrium models have proved inadequate to explain the observed strengths of [O II] and [N II] in case of planetary nebulae.

This paper is based on a Ph.D. thesis at the University of Wisconsin. The author expresses his gratitude to Professor Donald E. Osterbrock for suggesting the problem and for his constant guidance and encouragement throughout the course of this work. Special appreciation goes to Professor John S. Mathis for his supervision of this work at the final stage and to Drs. T. J. Bohuski and J. P. Cassinelli for fruitful discussions. The work was supported by a National Science Foundation grant to Professor Osterbrock. The computations were performed on the Univac 1108 of the University of Wisconsin Academic Computing Center. The author is grateful for a summer assistantship from the Space Astronomy Laboratory of the University of Wisconsin. The present support at the Indian Institute of Astrophysics is also acknowledged.

REFERENCES

Bell, K. L., and Kingston, A. E. 1967, *Proc. Phys. Soc.*, **90**, 31.
Bethe, H. A., and Salpeter, E. E. 1957, *Quantum Mechanics of One- and Two-Electron Systems* (New York: Academic Press).
Bohuski, T. J. 1973, *Ap. J.*, **183**, 851.
Brocklehurst, M. 1971, *M.N.R.A.S.*, **153**, 471.
———. 1972, *ibid.*, **157**, 211.
Brown, R. L. 1972, *Ap. and Space Sci.*, **16**, 274.
Brown, R. L., and Mathews, W. G. 1970, *Ap. J.*, **160**, 939.
Burbidge, G. R., Gould, R. J., and Pottasch, S. R. 1963, *Ap. J.*, **138**, 945.
Courtès, G., Louise, R., and Monnet, G. 1968, *Ann. d'Ap.*, **31**, 493.
———. 1969, *Astr. and Ap.*, **3**, 222.
Field, G. B., Rather, J. D. G., Aannestad, P. A., and Orszag, S. A. 1968, *Ap. J.*, **151**, 953.
Field, G. B., and Steigman, G. 1971, *Ap. J.*, **166**, 59.
Foukal, P. 1969, *Ap. and Space Sci.*, **5**, 469.
Henry, R. J. W. 1970, *Ap. J.*, **161**, 1153.
Hjellming, R. 1966, *Ap. J.*, **143**, 420.
Hummer, D. G., and Mihalas, D. 1970, JILA Report, No. 101.
Hummer, D. G., and Seaton, M. J. 1964, *M.N.R.A.S.*, **127**, 217.
Kahn, F. D. 1954, *B.A.N.*, **12**, 187.
Louise, R., and Sapin, C. 1973, *Ap. Letters*, **14**, 119.
Mathews, W. G. 1965, *Ap. J.*, **142**, 1120.
Mathews, W. G., and O'Dell, C. R. 1969, *Ann. Rev. Astr. and Ap.*, **7**, 67.
Morgan, W. W. 1972, private communication.
Morton, D. C. 1969, *Ap. J.*, **158**, 626.
Oort, J. H. 1954, *B.A.N.*, **12**, 177.
Oort, J. H., and Spitzer, L. 1955, *Ap. J.*, **121**, 6.
Osterbrock, D. E. 1971, *J. Quant. Spectrosc. and Rad. Transf.*, **11**, 623.
Peimbert, M., and Costero, R. 1969, *Bol. Obs. Tonantzintla y Tacubaya*, **5**, 3.
Pengelly, R. M. 1964, *M.N.R.A.S.*, **127**, 145.
Rubin, R. H. 1968, *Ap. J.*, **153**, 761.
Saraph, H. E., Seaton, M. J., and Shemming, J. 1969, *Phil. Trans. Roy. Soc. London, A*, **264**, 77.
Savedoff, M. P., and Greene, J. 1955, *Ap. J.*, **122**, 477.
Seaton, M. J. 1959, *M.N.R.A.S.*, **119**, 81.
Spitzer, L., Jr. 1948, *Ap. J.*, **107**, 6.
———. 1949, *ibid.*, **109**, 337.
Spitzer, L., Jr., and Savedoff, M. P. 1950, *Ap. J.*, **111**, 593.
Steigman, G., Werner, M. W., and Geldon, F. M. 1971, *Ap. J.*, **168**, 373.

DIPANKAR C. V. MALLIK: Indian Institute of Astrophysics, Hebbal, Bangalore-560006, India